

8 Reconsidering the Affinity between Metric and Tonal Structures in Brahms' Op. 76, No.8

Anja Volk (Fleischer)[†] and Elaine Chew^{*}

[†]Department of Information and Computing Sciences
Center of Content and Knowledge Engineering
University of Utrecht, Amsterdam, the Netherlands
anja.volk@meertens.knaw.nl

^{*}Epstein Department of Industrial and Systems Engineering
Hsieh Department of Electrical Engineering
Viterbi School of Engineering
University of Southern California
Los Angeles, California, USA
echew@usc.edu

Abstract

The relation between metric and tonal structures is a controversial subject in music theory. Brahms' music is well known for both its metric and harmonic ambiguities. According to David Lewin and Richard Cohn, Brahms' Capriccio Op. 76, No. 8 is characterized by a deep affinity between metric and tonal processes. We reconsider the study of this relation from the perspective of independent mathematical models, namely Inner Metric Analysis and the Spiral Array, to describe the metric and tonal domains. Inner Metric Analysis investigates the metrical structure expressed by the notes based on the active pulses of the piece rather than notated bar lines. In the case of the Capriccio, segments of metric characteristics similar to Lewin's and Cohn's findings are obtained. The Spiral Array Model consists of a three-dimensional realization of the *Tonnetz* that embeds higher-level tonal structures in its interior. When applied to the Capriccio, this model segments the piece into tonally stable sections that correspond to Lewin's and Cohn's observation. The comparison of the results of these models provides further evidence of the close relation between harmony and meter in Brahms' Op. 76, No. 8 proposed by Lewin and Cohn.

Tonal Theory for the Digital Age (Computing in Musicology 15, 2007), 138–171.

8.1 Background to Brahms' Capriccio Op. 76, No.8

8.1.1 Meter and Harmony in Music Theory

The description of the different forms of relations between metric and pitch processes is a challenging topic in music theory. According to Caplin (1983), most important theorists of the 18th and 19th centuries recognized a significant relationship between tonic harmonic function and metrical accentuation, but have little consensus on the nature of this relationship. Lewin (1981) and Cohn (2001) find a concrete and close relationship in Brahms' Capriccio Op. 76, No. 8. Brahms' compositions are characterized by complex metric processes implying different forms of hierarchies, displacements and ambiguities as discussed, for instance, in Schoenberg (1976), Epstein (1987), Frisch (1990), and Volk (2004).

This paper discusses the relation between meter and harmony in the piece from a different perspective. We apply the mathematical model of Inner Metric Analysis (Fleischer, Mazzola and Noll 2000, Nestke and Noll 2001, Mazzola 2002, Fleischer 2002, Volk 2004) and the mathematical model for tonal spaces of the Spiral Array (Chew 2000, 2006a, 2006b) to the Capriccio. The comparison of the results offers a new perspective on Lewin's (1981) and Cohn's (2001) findings about a deep affinity between meter and harmony in this piece.

8.1.2 Lewin's Analysis of Brahms' Op. 76, No.8

Lewin (1981) determines that the Capriccio contains, in the first 15 bars, the following metrical states: 6/4, 3/2 and 12/8. These metrical states are obtained by extracting from the left hand the lowest pitch of each arpeggio (see Figure 8.1) and grouping these notes according to the corresponding metric hierarchy of 6/4, 3/2 and 12/8 (see Figure 8.2). Lewin does not consider the complex metric structure of the right hand in his analysis. Each metrical state is associated with different sections as shown in Figure 8.2a. Bars 1–2 and 5–8 are assigned as 6/4 (red region), Bars 3–4 as 3/2 (blue region) and Bars 9–13 as 12/8 (green region). Furthermore, each region corresponds to a harmonic function: "tonic" (red), "subdominant" (blue) and "dominant" (green). Tonally, the example is largely divided into two halves: F (Bars 1–8) and e (a dominant-substitute key in Bars 9–15). Lewin assigns the last two bars as 12/8 but perceives in addition a metric modulation back to 6/4 within these bars, indicated with the light green color. Starting from this coincidence, Lewin develops mathematical arguments supporting a deep affinity between harmony and meter. Cohn extends Lewin's findings and characterizes the different metrical states by superimposed levels of pulses or motion that have conflicting periods.

Grazioso ed un poco vivace.
Annuthig lebhaft.

The image shows a musical score for the left-hand part of Brahms' Capriccio Op. 76, No. 8. The score is in 3/4 time and consists of five systems of two staves each (treble and bass clef). The left-hand part is marked with 'mp' and 'sust.'. The score is annotated with colored dots: red dots in the first system, blue dots in the second, red dots in the third, green dots in the fourth, and green dots in the fifth. The fifth system ends with a first ending bracket and a 'rit.' marking.

Figure 8.1. Notes of the left-hand part of Brahms' Capriccio Op. 76, No. 8 considered for the metric analysis by Lewin (marked with a dot), score reproduced from the first edition, published by Simrock in 1879. Courtesy of the McCorkle Brahms Cataloguing Project at the Department of Music, University of British Columbia.

1 m. of piece = $\frac{1}{2}$ of example

1 2 3 4 metric modulation

D D D D D

5 6 7 metric modulation (repeat) (1) etc.

prolongation →

Figure 8.2a. Metric and harmonic analysis of the Capriccio in Lewin (1981).

Grazioso ed un poco vivace.
Anmuthig lebhaft.

“tonic” **“subdom”**

“dominant”

p rit.

Figure 8.2b. Metric and harmonic segments of the Capriccio according to Lewin (1981).

8.2 Computational Models for Meter and Harmony

8.2.1 A Brief Literature Review

Computational models that assign a metric interpretation to a given piece of music are based on very different methods, such as rule-based approaches (Steedman, 1977; Longuet-Higgins and Lee, 1987; Povel and Essens, 1985), probabilistic models (Raphael, 2001), or oscillator models (McAuley, 1994; Large and Kolen, 1994; Large, 2000; Eck, 2002). Some of these models search for the main beat (Povel and Essens, 1985) while others search for the entire metric hierarchy (Temperley 2001, Toiviainen and Eerola 2004). The majority of computational metric models do not consider harmonic events for the assigning of the metric interpretation (an exception is Temperley, 2001). Since pitch information is mostly ignored, these models operate very differently in comparison to Lewin's analytic approach to the Capriccio, which is pitch-based. Furthermore, the relation between harmony and meter has been hardly investigated by computational models.

Similarly, computational models that assign a tonal interpretation to a given piece are based on diverse methods. Models for tonal recognition include Longuet-Higgins and Steedman's (1971) shape-matching algorithm based on the harmonic network, Krumhansl and Schmuckler's probe tone profile-matching method through computation of a correlation coefficient (see Krumhansl, 1990), Temperley's extensions on the K-S approach by modifying the original templates (1999) and by introducing Bayesian reasoning (2002), and Chew's (2001) center-of-effect generator (CEG) method that uses a nearest-neighbor search within the Spiral Array representation. Key-recognition methods form a critical step in systems for more complex tonal analysis, including local key finding (Schmulevich and Yli-Harja 2000, Toiviainen and Krumhansl 2003, and Sapp 2001), audio key finding (see, for example, Chuan and Chew 2007, Gómez 2006, and Izmirlı 2005), complete tonal analyses (Temperley 2002), tonal segmentation (Chew 2004, 2006a), and the generating of tree structures for tonal groupings (Rizo and Iñesta, 2005).

8.2.2 Inner Metric Analysis

Inner Metric Analysis is based on the idea of studying the meter of a work by considering all active pulses in a piece, not unlike Cohn's analysis of the Capriccio. These different levels of motion, pulses, or layers have been used in different music-theoretic approaches for the description of meter, such as by Yeston (1976), Lerdahl and Jackendoff (1983), and extensively by Krebs (1999). Inner Metric Analysis investigates the *inner metric structure* of the notes *inside* the bars, which is opposed to the normative state associated with the bar lines called *outer metric structure*. The model assigns *metric weights* to the notes that are generated from the superposition of the active pulses in the piece. A correspondence between the outer and inner metric structures results in what Fleischer (2002) terms *metric coherence*. The application of the model to Brahms' four symphonies in Fleischer (2003) and Volk (2004) has shown

that Brahms' music is often characterized by a lack of metric coherence, providing an explicit description of the discrepancies and ambiguities stated, for example, in Frisch (1990) and Epstein (1987).

We now give a brief introduction to the model; the details have been covered in Fleischer (2003) and Volk (2004). The general idea behind the model is a search for all pulses (chains of equally spaced events) of a given piece and the assigning of metric weights to each note of the piece based on the pulses that coincide at the note. The pulses considered by the model are based on note onsets. Figure 8.3 shows an example listing these pulses for measure 13 of the right hand of the Capriccio. The first row O under the notes shows the projection of the notes onto the set of all onsets. Within this set O we determine the pulses of the piece as subsets of equally spaced onsets that are maximal. A subset is maximal if it is not a subset of another subset consisting of equally spaced onsets. These maximal subsets are called *local meters*. Figure 8.3 lists all four local meters A , B , C and D of this example, indicated by dark circles. The local meters A and B consist of four onsets each, while C and D contain three onsets each. We call the number of onsets minus 1 the length k of a local meter, hence A and B have the length $k=3$, and C and D the length $k=2$. All local meters have different periods. A has a period of three, B has a period of one, C a period of two and D a period of four (as multiples of eighth notes). The triangles show the extension of each local meter throughout the entire piece with its specific period and phase. The extension continues a pulse after it has stopped until the end of the piece, and also backwards to the beginning of the piece.

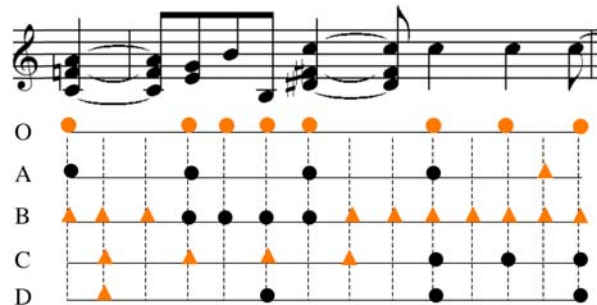


Figure 8.3. The set O of all onsets and all local meters of Bar 13 in the right hand.

Inner Metric Analysis makes the distinction between two different weights, namely the metric and spectral weights that consider the local meters and the extension of the local meters respectively. The metric weight is based solely on the local meters (the dark circles in Figure 8.3), while the spectral weight considers in addition the extension of each local meter (all dark circles and triangles in Figure 8.3). For each onset $o \in O$, the metric weight $W_{l,p}(o)$ sums the power function k^p of the length k of all local meters m that have a minimum length l and coincide at o :

$$W_{l,p}(o) = \sum_{\{m \in M(l); o \in m\}} k^p$$

The spectral weight $SW_{l,p}(t)$ considers in addition the extension of all local meters that coincide at t :

$$SW_{l,p}(t) = \sum_{\{m \in M(l); t \in ext(m)\}} k^p$$

Figure 8.4 displays the results for the short example in Figure 8.3 using different values for the weighting parameter p . The x-axis represents the time axis; the background marks the notated bar lines. The higher the line, the higher the corresponding weight. While both the metric and spectral weights using the parameter $p=2$ do not exhibit a regular pattern, the spectral weight $SW_{2,4}$ in the rightmost picture is characterized by two different weight layers. The highest layer is built upon every third eighth note in this example. Hence in this short example, the inner metric structure differs from the outer metric structure of the accent hierarchy of the notated 6/4, which has large metric accents on the first and fourth quarter notes of each bar. This is not a surprising result, however, given the numerous syncopations in this excerpt. Increasing the value of p leads, at least for the spectral weight, to the emergence of layers. We will discuss the different contributions of the metric and spectral weights to segmentation processes in the metric domain below.

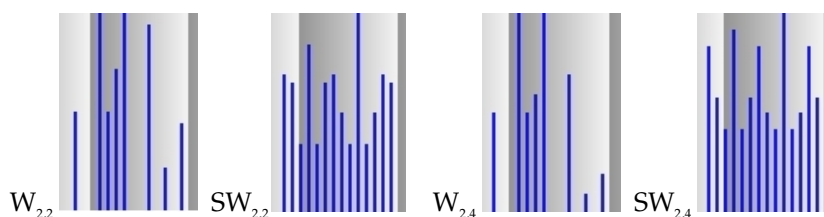


Figure 8.4. Metric and spectral weights for Bar 13 using different parameters p . The first two pictures from left display the metric and spectral weights for $l=p=2$; the last two pictures display the metric and spectral weights for $l=2$ and $p=4$.

8.2.3 The Relation between the Inner and Outer Metric Structures

Inner Metric Analysis describes the inner metric structure generated by the notes inside the bar lines without considering the outer metric structure associated with the time signature. The previous example demonstrated that these structures may differ from each other. Figure 8.5 gives an example in which the weight layers of the inner metric structure coincide with the typical hierarchical layers of the outer metric structure. The spectral weight $SW_{2,2}$ of the first movement of Beethoven's Sonata Op. 31, No. 1, in 2/4 meter, shows four distinctive layers. The spectral weights on the first beats of all bars build the highest layer, while those of the second beats of all bars create the second highest layer. The weights on the second and fourth eighth notes

build a lower layer, while those on the weak sixteenth notes in between create the lowest layer.

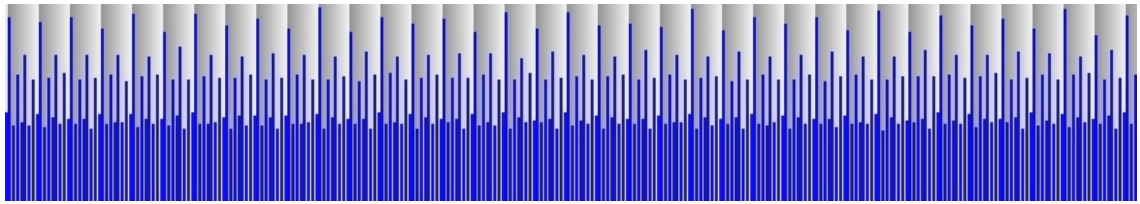


Figure 8.5. Excerpt from the spectral weight $SW_{2,2}$ of the first movement of Beethoven's Sonata Op. 31, No. 1 (time signature: 2/4).

Such a correspondence between the inner and outer metric structures reflects the fact that the metric structure of the notes respects the normative state of the bar lines. We call such a relationship metric coherence (Fleischer [Volk] 2003). One might expect that such a relation is the normal case. However, music theorists have discussed many examples where the structure implied by the notes contradicts the abstract grid of the bar lines.

The first movement of Schumann's Third Symphony, in 3/4 time, is one such well-known example characterized by a discrepancy between the inner and outer metric structures (see Epstein 1987 and Krebs 1999). The excerpt from the spectral weight of the first violins in this movement in Figure 8.6 shows weight layers that do not coincide with the metric hierarchy implied by the notated bar lines. In every other measure, the highest metric weight is not located on the first beat, but on the second. Hence metric coherence does not occur in this example. The model thus confirms Epstein's and Krebs' observations about a discrepancy between the notes and the abstract grid of the bar lines. Lewin's analysis of Brahms' Capriccio points to another example characterized by complex metric processes that do not necessarily coincide with the notated time signature. We will investigate this phenomenon in detail in section 8.3.

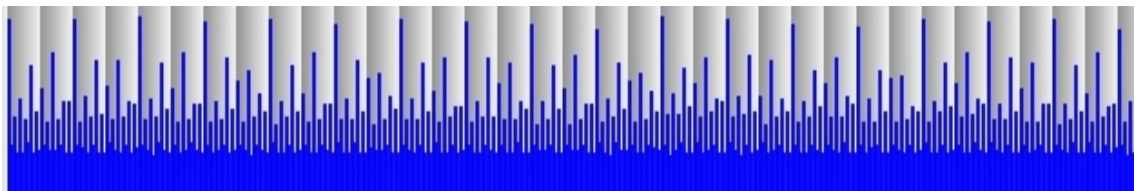


Figure 8.6. Excerpt from the spectral weight $SW_{2,2}$ of the first violins in the first movement of Schumann's Third Symphony (time signature: 3/4).

8.2.4. Global vs. Local Structures in Inner Metric Analysis

This section provides the basis for the segmentation processes using Inner Metric Analysis to be introduced in Section 8.2.6. Lewin's analysis of the Capriccio identifies

different segments of tonal and metric stability in the first 15 bars of the piece. The application of Inner Metric Analysis to the piece in section 8.3.1 hence focuses on the determination of metrically stable segments.

Segmentation processes based on tonal structures have been investigated in the music theory literature to a much greater extent than those dealing with the metric domain (see, for example, Temperley 2001, Chew 2004, and Honingh 2007). Different tonal keys often characterize the different thematic sections of a sonata, and hence can be indicators of significant boundaries. It is important to note that areas of transition could exist wherein no clear tonality can be found.

In Chew (2004), the Argus method was introduced as a way to track degrees of change in the tonal context using two consecutive windows of musical information. Segmentation boundaries are then detected as statistically significant peaks in the tonal distance function. This method will be discussed in greater detail in Section 8.2.5 before it is employed in the analysis of the Brahms Capriccio in Section 8.3.2.

Similarly, we search in the metric domain for segments characterized by stable metric layers, having similar weight profiles, using Inner Metric Analysis. However, not all pieces are characterized by metric weights with stable layers (see Fleischer 2003), hence for pieces with no stable regions, other criteria for segmentation processes have to be defined. In this article we consider only cases where regions of stable layers occur.

Inner Metric Analysis of an entire piece considers all possible relations between all onsets of the piece, even the relation between the very first and very last onsets. The analysis of isolated segments may therefore result in different metric characteristics, compared to the analysis of a segment as part of the entire piece, if relations to onsets outside of this segment have a high influence on the metric weight within the segment. Our search for stable segments starts from the analysis of the entire piece using the full amount of metric information, and proves the inner stability of the segments in a second step by analyzing the isolated segments. As we will see later, adjustments of the boundaries of segments may be necessary within this second step.

The metric and spectral weights contribute differently to our segmentation procedure. The spectral weights of Figures 8.5 and 8.6 show very constant weight layers throughout the entire piece, which is frequently a characteristic of the spectral weight. The metric weight is in general more sensitive to local changes of the metric structure and reacts with changes in the weight layers. Hence, the extension of all local meters in the spectral weight approach allows for the global characterization of the predominant metric structure of a piece or a segment; the metric weight reflects a more local perspective, and can determine boundaries between different segments.

Beethoven's Sonata Op. 31, No. 1 gives an example of the different behaviors of the metric and spectral weights concerning robustness and sensitivity. Figure 8.7 shows four excerpts from the metric weight profile of the first movement of Beethoven's

Sonata Op. 31, No.1. While the spectral weight in Figure 8.5 is characterized by four different layers, the number of layers in the metric weight changes throughout the piece. Only the excerpt from the second theme in the exposition, profile given in Figure 8.7b, shows different layers in the last four bars (first beats of the bars, second beats of the bars, second and fourth eighth notes, sixteenth notes in between). The excerpts from the first theme in the exposition (Figure 8.7a) and the recapitulation (Figure 8.7d) are characterized by large weights on the first beats of the bars, followed by the weights on the second beats in some bars. Furthermore, the metric characteristic of the first theme in the recapitulation is different from the exposition in that the beginnings of the bars reveal a hypermeter of two bars due to greater metric weights on the first beat of every second bar. The third excerpt (Figure 8.7c) is characterized by large metric weights on the first beats of all bars as well, but the second beats do not generate a stable second layer, since in many bars the third or seventh eighth note tends to converge on the weight of the second main beat. Hence, the number of weight layers for the metric weight changes throughout the piece, in contrast to the spectral weight, which exhibits constant layers.

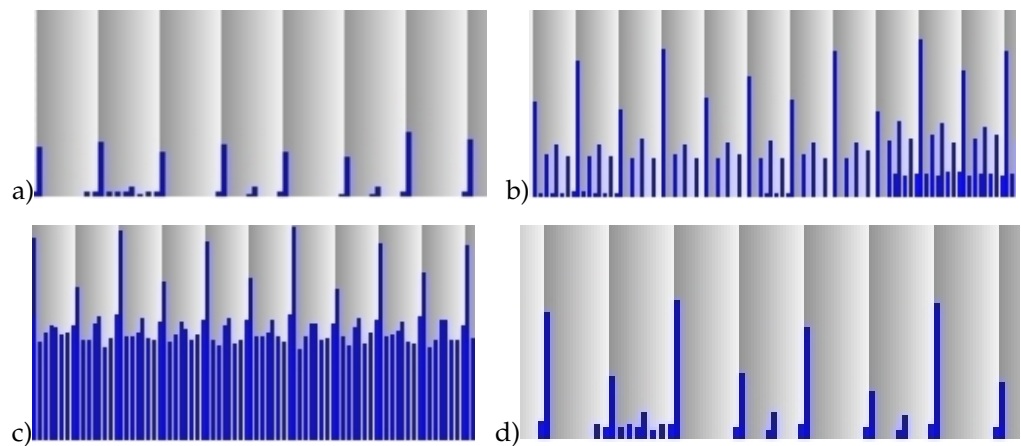


Figure 8.7. Excerpts from metric weight $W_{2,2}$ of the first movement of Beethoven's Sonata Op. 31, No. 1: **(a)** Bars 1–7 (first theme in exposition), **(b)** Bars 64–74 (second theme in exposition), **(c)** Bars 133–43 (development), and **(d)** Bars 200–7 (first theme in recapitulation).

Changes in the layers of the metric weight can indicate meaningful segments in the piece. In comparison to tonal segmentation, segmentation in the metric domain has been much less extensively studied. Existing research focuses on finding the main beat or determining the overall metric hierarchy. Little effort has been spent on devising strategies for determining the local time structure or segmentation boundaries. In the following paragraphs we show further examples of metric weights that illustrate how the change in the metric weight layers corresponds to segments assigned by music theorists.

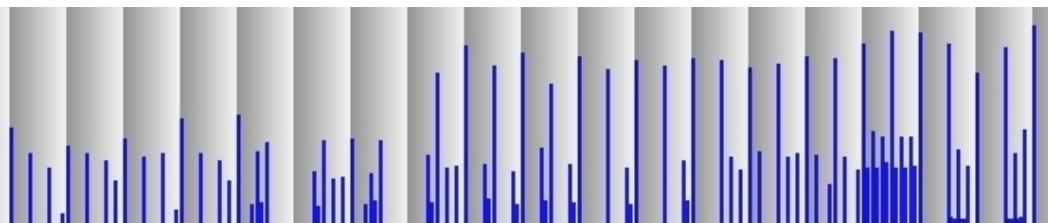


Figure 8.8. Excerpt from metric weight $W_{2,2}$ of the first violins in the first movement of Brahms' Third Symphony (Bars 3–21).

Considerable change in the metric weight layers occurs in the opening of the first movement of Brahms' Third Symphony, noted with a 6/4 meter. Figure 8.8 gives an excerpt for the beginning of the metric weight of the violins (see score in Figure 8.9). Bars 1–4 of this excerpt (which correspond to Bars 3–7 of the score) do not exhibit the typical 6/4 metrical hierarchy, with large metric weights on the first and fourth quarter notes. Instead, the first, third and fifth quarter notes are assigned large weights.



Figure 8.9. The violin part of the first movement of Brahms' Third Symphony (Bars 3–21). The violins start the theme in Bar 3 of the score, hence the first bar of the metric weight corresponds to the third bar in the score. Our references to bars within the metric weight assume Bar 1 for the first analyzed bar.

These peaks correspond to the metric profile characteristic of a 3/2 meter. Beginning in Bar 7 of the excerpt (and more evident in Bar 9), large weights are located on either both the first and fourth beats, or only on the fourth beat, as is typical for a 6/4 meter. Starting at the second half of Bar 8, a considerable shift in the highest layer toward larger weights is introduced, and a correspondence to a 6/4 metric profile becomes evident. This result obtained from the metric weight corresponds to an observation stated by Walter Frisch:

The main theme, entering in the violins in the third bar, begins to project a metrical profile, but one that fits more clearly into 3/2 than 6/4. Only in Bar 7 is the duple division of the bar firmly supported in all parts: the theme, the 'motto', and the harmonic voices move every half bar (Frisch 1990: 156).

A similar situation occurs in Brahms' Violin Sonata Op. 78 (notated in 6/4). Figure 8.10 shows the excerpt from the metric weight of the violin for the beginning of the piece. Bars 10–19 again exhibit a metric characteristic that reflects a 3/2 meter, with large metric weights on the first, third and fifth quarter notes, while the bars before and after this section correspond to a 6/4 meter, with large metric weights on the first and fourth quarter notes of the bars. Cohn characterizes these different sections as the principal thematic material before Bar 10, followed by a transitional passage that is metrically dissonant to the opening bars which is dissolved with the return of the main theme in Bar 21.

The movement opens in the state of metric consonance. A transitional passage culminates in a dominant prolongation at Bar 16, which leads to a modified counter-statement of the opening material at Bar 21. The dominant prolongation is in a state of double hemiola. In these bars, both violin and piano are indirectly dissonant with the opening metric consonance.... The resolution of the metric dissonance coincides with the return of the tonic and of the principal thematic material (Cohn 2001: 305).

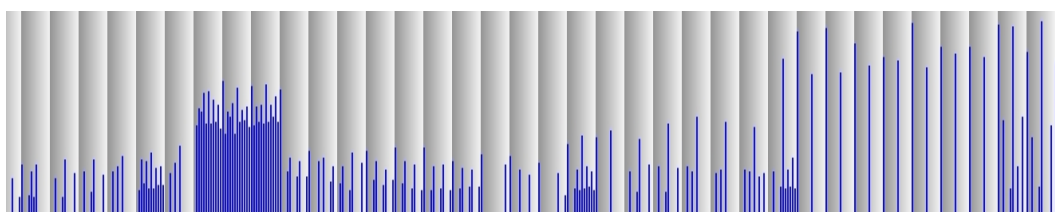


Figure 8.10. Excerpt from metric weight $W_{2,2}$ of the violin in the first movement of Brahms' Violin Sonata Op. 78.

Hence, the different types of layer profiles of the metric weight can be used for segmenting a piece into different sections, as in this case segmenting the piece between the main thematic material and the transition.

The metric weight of the exposition of the first movement of Brahms' Second Symphony in 3/4 indicates sections that coincide with tonal segments of the exposition. Figures 8.11 to 8.13 display excerpts of three different sections of the weight that demonstrate different metric characteristics. In the first section (Figure 8.11) the highest metric weights are located on the first beats of the bars. The second section (Figure 8.12) reveals layers that correspond to a 4/4 meter instead of a 3/4 meter. The last section (Figure 8.13) shows little differentiation between the highest layer and other layers of the weights of the main quarter notes of the bars. These three sections correspond to the three segments of a tonal analysis of this exposition (Phipps 2001).

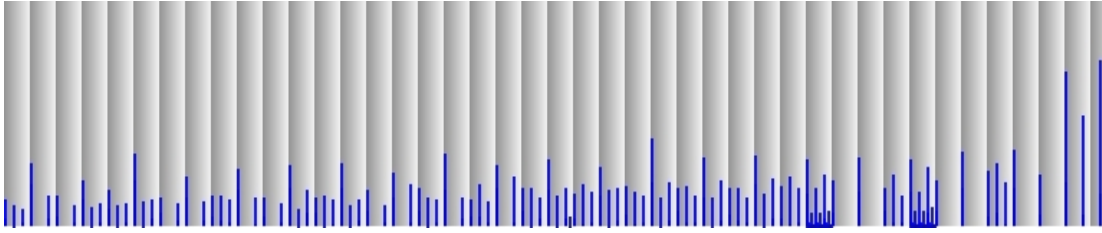


Figure 8.11. Excerpt from metric weight $W_{2,2}$ of the exposition of the first movement of Brahms' Second Symphony, Bars 1–43.

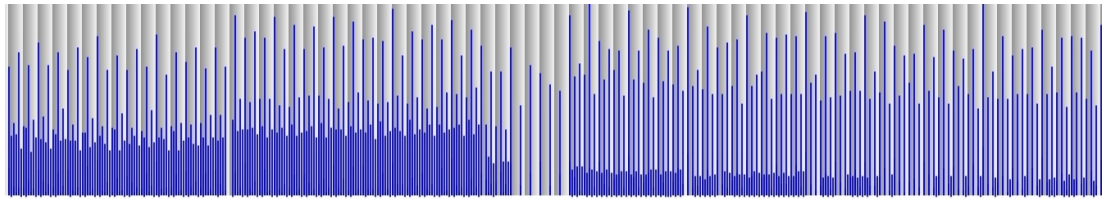


Figure 8.12. Excerpt from metric weight $W_{2,2}$ of the exposition of the first movement of Brahms' Second Symphony, Bars 44–117.

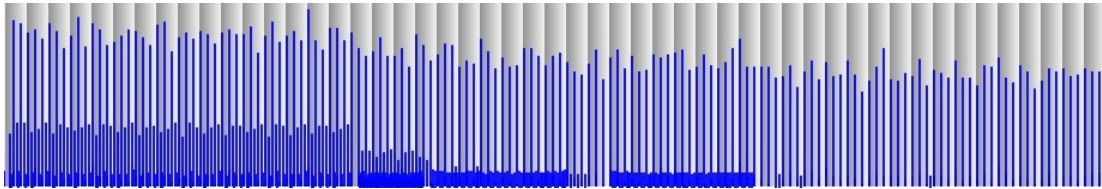


Figure 8.13. Excerpt from metric weight $W_{2,2}$ of the exposition of the first movement of Brahms' Second Symphony, Bars 118–86.

8.2.5 Determining of Tonally Distinct Segments Using the Spiral Array

At this point, we digress from metric models to briefly describe the Argus algorithm (Chew 2004, 2006b) mentioned earlier, a method for determining segmentation boundaries based on tonal contexts. The Argus method represents a recent application of the Spiral Array (Chew 2000) to the determining of sections of music with distinct pitch collections. A different method, based on an optimization approach, was proposed in Chew (2002).

The Spiral Array is a geometric model that represents pitches on a spiral such that spatially close pitch representations form higher-level tonal structures such as triads and keys. These higher-level structures are, in turn, represented by spirals embedded in the interior of the outer pitch-class spiral. The Argus algorithm uses only the outermost pitch-class spiral, but an algorithm for key finding uses the pitch-class and the pair of key spirals. A more detailed description of the Spiral Array and comparisons of its structure to Krumhansl's and Lerdahl's geometric representations of tonality can be found in the article by Chew in this issue.

The pitch-class spiral, shown in Figure 8.14, is a three-dimensional realization of the Tonnetz. Unlike the Tonnetz, the Spiral Array summarizes collections of pitches as points in its interior, called centers of effect (c.e.'s). By mapping a musical selection to its center-of-effect, and conducting a nearest-neighbor search for the closest key representation, we can determine the key of the selection. This center-of-effect generator (CEG) method has been shown to be a useful technique for key recognition (see Chew 2001; also Ch. 4).

The center-of-effect plays an important role in the Argus algorithm. It has been shown to be an effective surrogate for the tonal context (Chew and Chen, 2003). Consider the illustration in Figure 8.14. When comparing pitch collections from two consecutive segments of music, the distance between their centers-of-effect quantifies the tonal difference between the two musical selections. The magnitude of this distance can thus be used as an indicator of the likelihood that a tonal boundary exists between the two selections. The resulting time series of these computed distances contains numerous peak values. The statistical method from process control is then invoked to determine when a peak is significant and worth noting. This method assumes that the distance values can be modeled using a normal distribution.

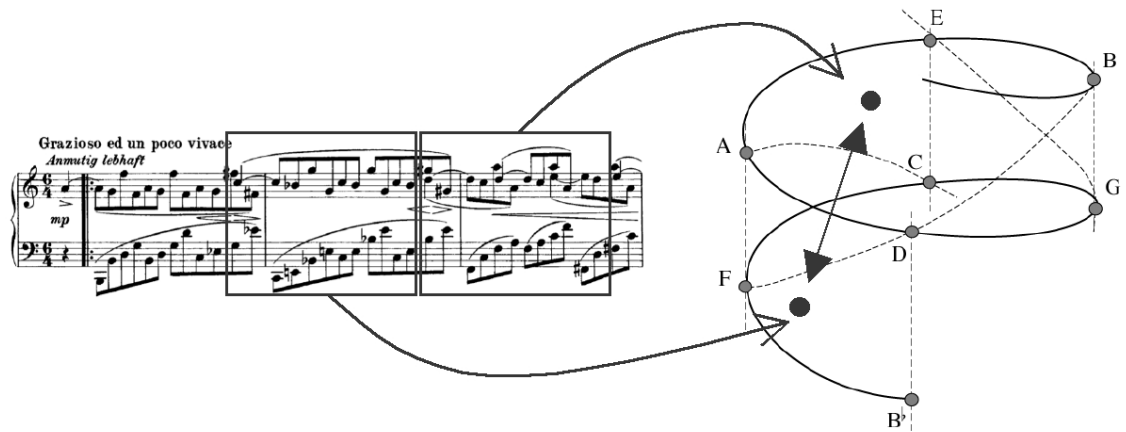


Figure 8.14. Distance between centers of effect (summary points) inside the Spiral Array provides tonal distance between consecutive segments of music.

The Argus has been applied successfully to musical examples by Schubert and MacDowell (Chew 2006a), and Messiaen (Chew 2004). We reproduce the chart for one of the Messiaen analyses here in Figure 8.15 using equal forward and backward window sizes of 60 ($= f = b$) sixteenth notes. The bar at the top of the chart shows the sections in the piece, as indicated by section headings in the score penned by the composer. The solid horizontal line marks the average distance, μ , while the dotted horizontal lines mark the levels $\mu + \sigma$ and $\mu + 2\sigma$ respectively. Note that, in this example, all peaks above $\mu + \sigma$ correspond to points at or close to significant section boundaries.

The two peaks above $\mu+2\sigma$ correspond to the transition between sections A and C. More detailed analyses of the behavior of the distance values time series as the window gets smaller can be found in Chew (2006b).

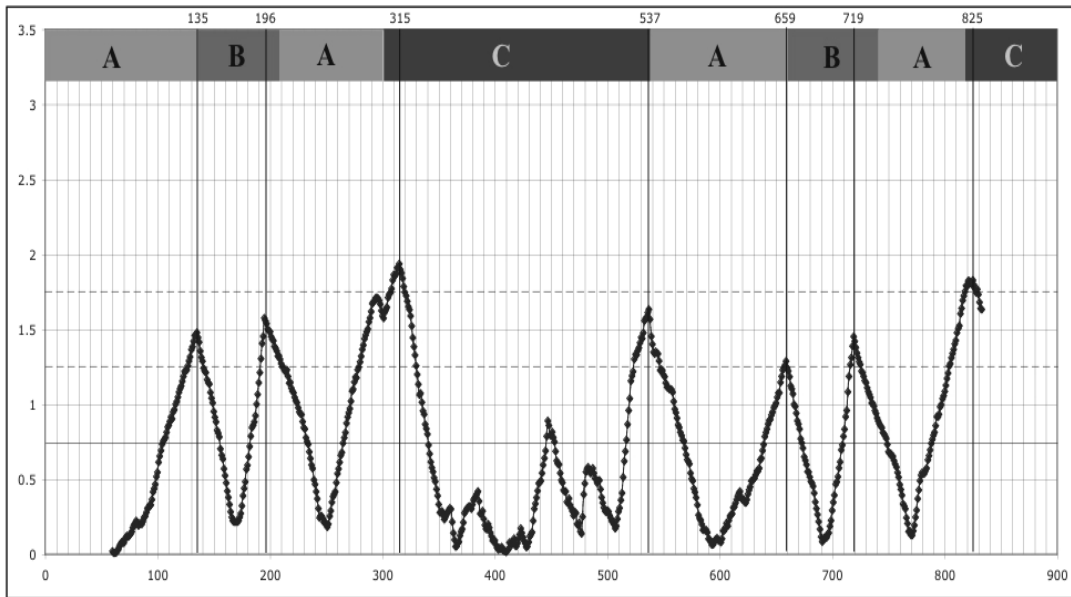


Figure 8.15. Analysis of segmentation boundaries in Messiaen's *Vingt Regards, No. 4*, using the Argus algorithm with the parameters $f = b = 60$, $\mu = 0.7418$, $\sigma = 0.5083$.

The results of the analysis of Brahms' tonally ambiguous Capriccio are given in Section 8.3.2. This analysis will provide some evidence for the affinity between tonal and metric structures in the piece.

8.2.6 Determining of Metrically Distinct Segments Using Inner Metric Analysis

In this section, we introduce a two-step process for the determining of metrically distinct segments. The first part, like the Argus method, uses a distance function (in this case, the correlation coefficient) to determine the similarity between consecutive bars in the metric profile. The second part isolates and investigates the segments identified in step one to confirm their metric profiles.

As shown in Section 8.2.4, the sensitivity of the metric weight is able to indicate sections that are characterized by different metric layers that correspond to meaningful segments of the piece. A possibility for the automatic extraction of these sections is the measurement of the similarity of the metric weight of consecutive weight segments using the correlation function. In this case, the correlation function serves as the distance measure for metric similarity between two consecutive windows of time, say, one bar. The correlation of the metric weight of two consecutive Bars should be

high in stable regions of metric coherence; it should drop to a lower level whenever the second bar introduces a different metric characteristic. Other segment sizes (such as half bars) could be considered. A change between high and low coefficient values indicates a boundary between stable regions of differing weight layers, or between stable and unstable regions.

Figure 8.16 gives an example of correlation coefficient values of the metric weight of consecutive bars for the analysis of the violins in Brahms' Third Symphony (see metric weight in Figure 8.8). The i -th column in Figure 8.16 indicates the correlation coefficient value between the metric weights of Bar i and Bar $i+1$ of the segment. Since the metric weight is defined only on note onsets o , we define the metric weight of all silence events s (based on the finest grid of the piece) as zero, and hence obtain for each bar the same number of events in the accent profile. Let $\{x_i : i = 1, \dots, n\}$ and $\{y_i : i = 1, \dots, n\}$ be the accent profiles of two consecutive bars. We use the following correlation coefficient formula for the measurement of the similarity of the metric characteristics of the two bars:

$$r = \frac{\sum x_i y_i - n \bar{x} \bar{y}}{\sqrt{\sum (x_i - \bar{x})^2} \sqrt{\sum (y_i - \bar{y})^2}}$$

The graph of the correlation coefficient values shown in Figure 8.16 reaches high values in the beginning, drops to a lower level at the pair of consecutive Bars 4 and 5 and increases again to a higher level beginning with the consecutive Bars 9 and 10. The green line marks the threshold $\mu - \sigma$ of the mean value μ of all correlation coefficient values and their standard deviation σ . The decrease of the five values under this line, beginning at the 4th data point, shows that this decrease is significant (assuming that the correlation coefficient values can be approximated by a normal distribution). For the determination of segment boundaries we will consider values that drop under this threshold.

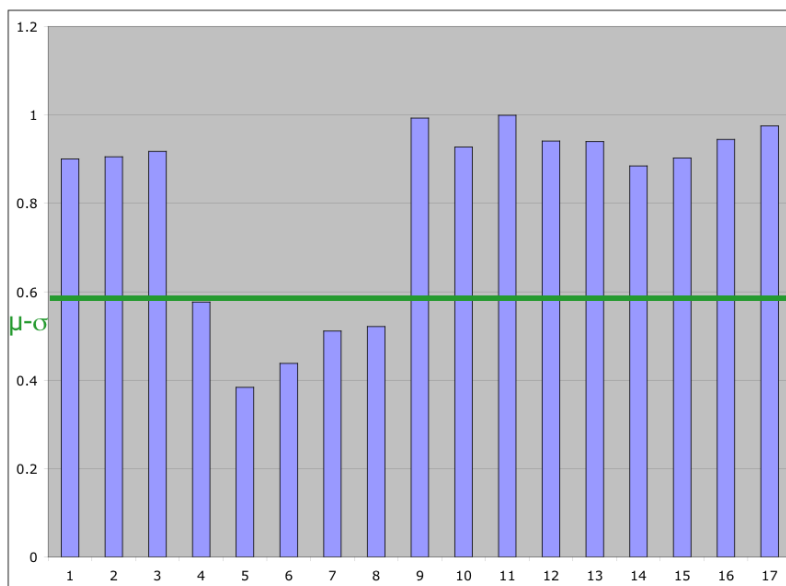


Figure 8.16. Correlation coefficient values between metric weights of consecutive bars for the analysis of the violin part (Bars 3–21) of Brahms’ Third Symphony, first movement (Bars 1–18 of the metric weight).

Hence, the correlation coefficient values indicate three segments: the first stable segment with high similarity between metric weights of consecutive bars terminates at the end of Bar 4, followed by an unstable region characterized by low similarity between the metric weights of consecutive Bars, followed by a second stable segment starting at Bar 9 with high correlation coefficients. The first stable region is characterized by a 3/2 profile; the second stable region has a 6/4 profile (see Figure 8.8). Hence, the unstable region between these segments could be interpreted as a transition between these two states. Figure 8.17 highlights these three segments with different colors.

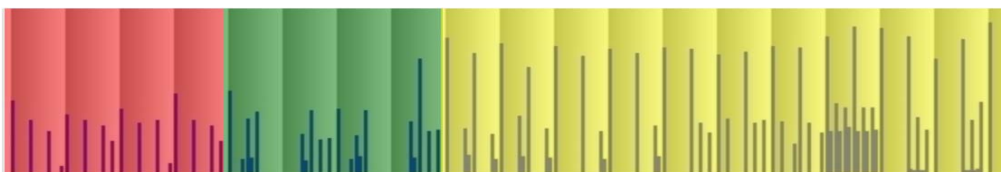


Figure 8.17. Segmentation of the metric weight of Brahms’ Third Symphony, first movement (Bars 3–21), according to the correlation coefficient values.

In the second step we analyze the isolated segments in order to test their boundaries after excluding the influence from outside the segments. Furthermore we check whether the instability (the lack of stable weight layers reflected by low correlation coefficient values) of the transitional passage in Bars 5–8 is due to the influence of the

surrounding segments of differing metric weight layers. Conflicting layer contexts might prevent the emergence of stable weight layers within this passage. Hence, neglecting the relations of the onsets within this passage to the surrounding context might lead to stable layers within the isolated analysis.

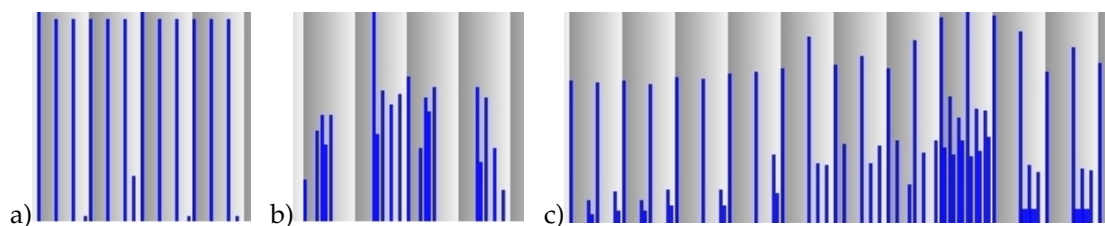


Figure 8.18. Metric weight of the isolated segments; **(a)** Bars 1–4, **(b)** Bars 5–8, and **(c)** Bars 9–18.

The metric weight of the isolated segments in Figure 8.18 confirms the 3/2 characteristic of the first segment with high metric weights on the first, second and third half notes of the bars, and the 6/4 characteristic of the third segment. The transitional second passage does not gain stable weight layers within the isolated analysis, hence it remains a transitional unstable passage between two stable segments. The spectral weights of these isolated segments that yield the predominant metric characteristic of each segment in Figure 8.19 confirm these results. While the spectral weight of the first segment assigns large weights to the main half notes of a 3/2, the transitional passage does not exhibit stable layers. The spectral weight of the last segment confirms the 6/4 characteristics.

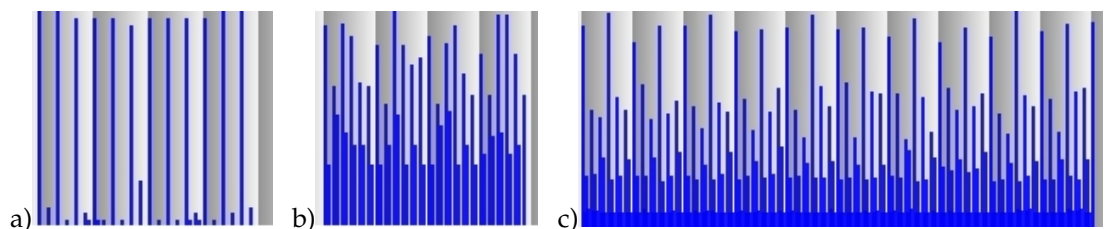


Figure 8.19. Spectral weight of the isolated segments; **(a)** Bars 1–4, **(b)** Bars 5–8, and **(c)** Bars 9–18.

The correlation coefficient values of the stable first and third segments are above the $\mu-\sigma$ threshold, which indicates that the segments are also metrically stable from the inside perspective that neglects the influence of the surrounding contexts. An attempt to enlarge the stable segments by choosing Bars 1–5 (instead of Bars 1–4) as a candidate for the first segment, and Bars 8–18 (instead of Bars 9–18) as a candidate for the third segment, results in significantly low correlation coefficient values for the pair (Bar 4, Bar 5) and the pair (Bar 8, Bar 9). Hence, no readjustments of the segment boundaries are necessary within this second step. Bars 1–4 constitute the maximally stable first segment, and Bars 9–18 the maximally stable third segment.

We apply this segmentation procedure consisting of two steps (apply correlation coefficient values of consecutive bars to the metric weight of the entire piece first, then investigate the isolated segments as a second step) to Brahms' Capriccio in section 8.3.1.

8.3 Brahms' Op. 76, No. 8 Revisited

8.3.1 Metric Analysis

In this section we describe the metric characteristics of the first 15 bars of the Capriccio according to Inner Metric Analysis and segment the piece into metric regions.

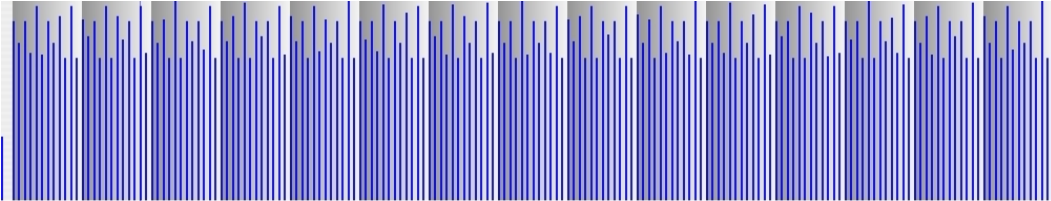


Figure 8.20. Metric weight $W_{2,2}$ of both hands of Bars 1–15.

The onsets of the left and right hand parts together perform an almost continuous eighth note pattern through the piece with the exception of the first quarter note at the very beginning. Hence, the corresponding metric weight in Figure 8.20 reveals a differentiation of the metric weight into only two metric layers. The higher layer is built upon the six main beats of all bars, the lower layer upon the weak eighth notes in between. These layers are stable throughout the entire section of Bars 1–15; no segments can be derived from the metric weight of both hands.

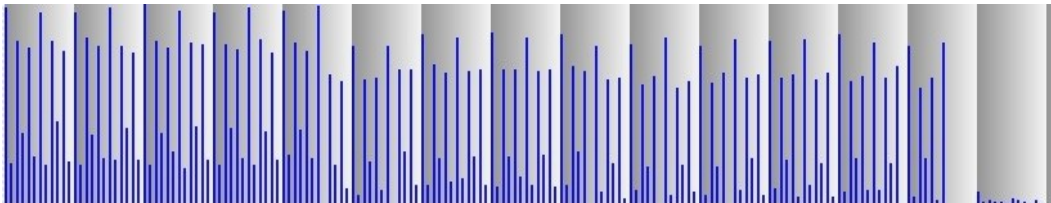


Figure 8.21. Metric weight $W_{2,2}$ of the left hand.

Analyzing the left and right hand parts separately results in different metric layers. Figure 8.21 displays the metric weight $W_{2,2}$ of the left hand part. The metric weight is highest at the 1st and 4th quarter notes of the bars; the weights of the 2nd, 3rd, 5th and 6th quarter notes form a second layer. The lowest layer consists of the weights of the weak eighth notes in between. Hence, the metric hierarchy associated with a 6/4 meter is reflected within the inner metric structure of the left hand in the section containing all bars from Bar 1 to the first half of Bar 14. The overall level of all weights drops slightly in Bar 6 although the characteristic of a 6/4 is maintained until Bar 14. In Bar 15 all weights drop to a very low level. The predominant metric structure in

Bars 1–15 according to the spectral weight of the left hand part is that of a 6/4 (see Figure 8.22).

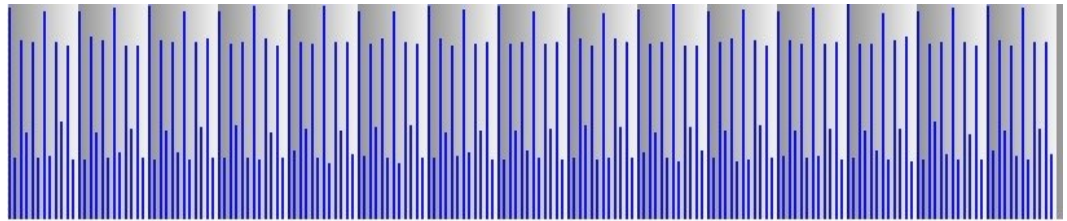


Figure 8.22. Spectral weight $SW_{2,2}$ of the left hand.

The observed local changes of the metric weight raise the question of whether the correlation coefficient would indicate a segment boundary between Bars 5 and 6, and after Bar 14. Figure 8.23 shows the correlation coefficient values for the metric weights of consecutive bars of the left hand. The values do not drop under the $\mu-\sigma$ threshold at the pair of Bars 5:6, hence the overall decrease of all metric weights to a lower level does not indicate a boundary at this point. The correlation coefficient values for the pair of Bars 13:14 and the pair of Bars 14:15 are lower than the threshold, and indicate a less stable segment starting in Bar 14 after the stable segment of Bars 1–13.

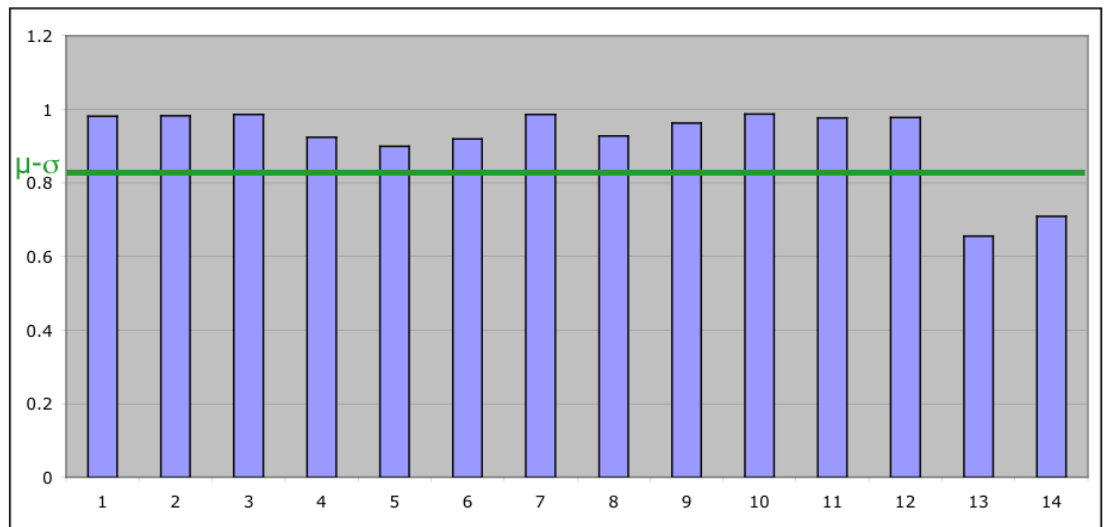


Figure 8.23. Correlation between metric weights $W_{2,2}$ of consecutive bars for the analysis of the left hand.

In the second step of our segmentation process we consider the metric weights of the isolated segments (Bars 1–13 and Bars 14–15). Figure 8.24 shows that the unstable second segment also remains unstable without the influence of the first stable segment.

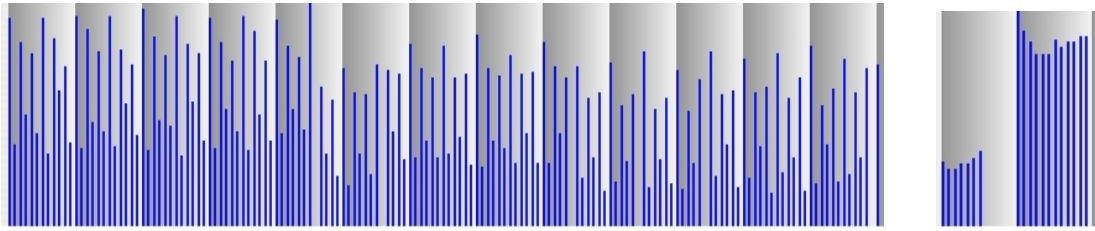


Figure 8.24. Metric weights $W_{2,2}$ of the isolated segments Bars 1–13 (left) and Bars 14–15 (right).

The test whether a more stable second segment can be obtained by a slight change of the boundary (the enlargement of the second segment by one bar) does not result in stable weight layers for the segment candidate of Bars 13–15 (see Figure 8.25), even though the beginning is characterized by alternating high and low weights. The correlation coefficient values of consecutive bars remain low (0.48 and 0.32). Hence, a readjustment of the boundaries within the second step of the isolated analyses of the segments is not necessary. The left hand part of Bars 1–15 of the Capriccio is therefore divided into two segments; the stable first segment of Bars 1–13 with its weight layers corresponding to a 6/4 pattern, and the unstable second segment of low correlation coefficient values of Bars 14–15. This very short segment corresponds to the region of metric modulation according to Lewin's analysis of the left hand.

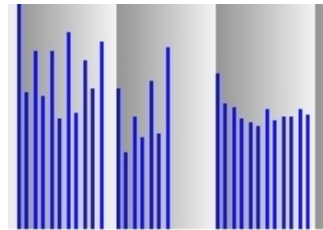


Figure 8.25. Metric weights $W_{2,2}$ of Bars 13–15.

The predominant inner metric structure of the right hand according to the spectral weight in Figure 8.26 is characterized by a highest layer of the weights of the 2nd, 6th and 10th eighth notes of the bars. These three peaks indicate a characteristic shifted 3/2 pattern, instead of a 6/4 pattern as observed in the analysis of the left hand. The shift is due to the many syncopations in the right hand.

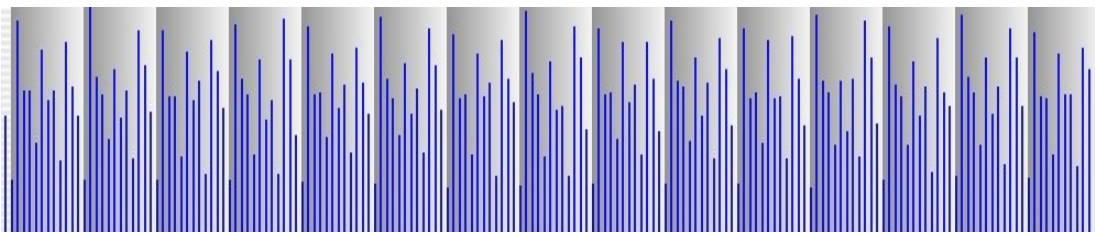


Figure 8.26. Spectral weight $SW_{2,2}$ of the right hand.

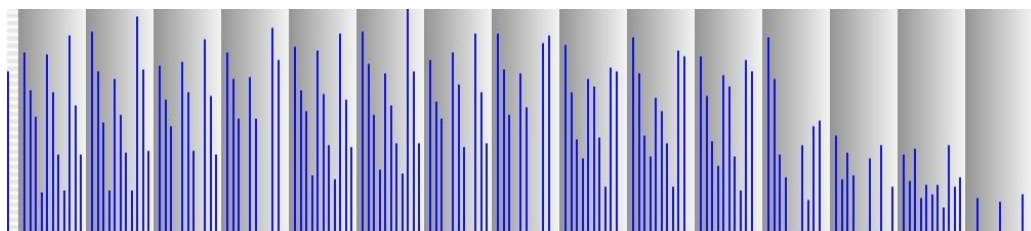


Figure 8.27. Metric weight $W_{2,2}$ of the right hand.

The metric weight in Figure 8.27 demonstrates that this predominant metric pattern is not present in all bars of this section, according to a more local perspective on the inner metric structure. Starting in Bar 12 these peaks disappear. The corresponding correlation coefficient values in Figure 8.28 show a drop under the $\mu-\sigma$ threshold starting at the pair of Bars 11:12, with one value above the threshold at the pair of Bars 13:14. According to these values we could conclude that there are four segments: the very stable first segment with a high similarity between consecutive bars consisting of Bars 1–11, the second segment consisting of Bar 12 only, the third segment of Bars 13–14 as a relatively stable segment of higher correlation coefficient values, and the fourth segment consisting of Bar 15.

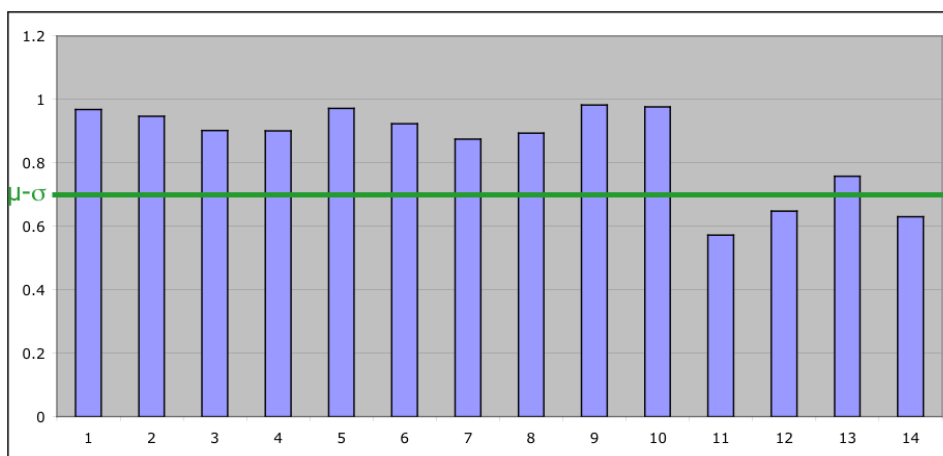


Figure 8.28. Correlation between metric weights $W_{2,2}$ of consecutive bars for the analysis of the right hand part of Bars 1–15.

Figure 8.29 shows the isolated analyses of these segments. Peaks at the 2nd, 6th and 10th eighth notes in the entire segment characterize the stable section—the first segment (from Bar 1 to Bar 11) of high correlation coefficient values. The general level of the weights drops in the last three bars to a slightly lower level. The second segment of Bar 12 is characterized by four peaks: at the 2nd, 5th, 8th and 11th eighth notes. The third segment of Bars 13–14 is stable only in Bar 14, characterized by two weight layers of alternating high and low values, and having a low correlation coefficient

value ($r=0.68$). The last segment of Bar 15 shows large metric weights on the 2nd, 4th and 6th quarter notes. However, the low correlation coefficient value of the isolated third segment, which resulted in three short segments in the last section of Figure 8.28, is not satisfactory. The correlation coefficient values of Bars 13:14 within the analysis of the entire piece were above the $\mu-\sigma$ threshold, indicating a high degree of similarity between these two bars. A high similarity is not replicated in the isolated analysis of these bars. Furthermore, a result having three consecutive very short segments of only one or two bars each is not a very intuitive one.

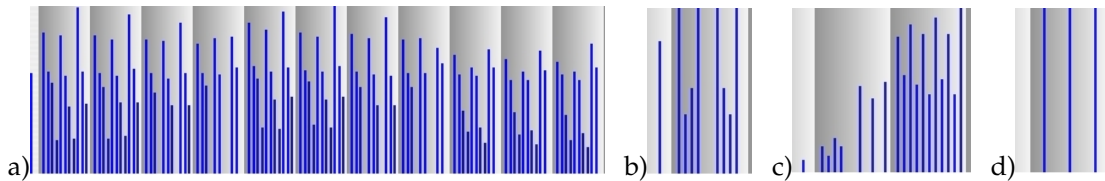


Figure 8.29. (a) Metric weight $W_{2,2}$ of Bars 1–11, (b) Bar 12, and (c) Bars 13–14, and (d) Bar 15.

Therefore, even though the correlation coefficient of the pair of Bars 13:14 is slightly above the threshold with respect to the analysis of the entire piece, we construct from the last three short segments one greater segment consisting of Bars 12–15. Hence we obtain two segment candidates of Bars 1–11 and Bars 12–15. The corresponding isolated analyses of these two segments are shown in Figure 8.30.

The isolated analyses of the two segment candidates shown in Figure 8.30 reveal, for the second segment, no stable weight layers. The correlation values of these consecutive bars are very low: 0.54, 0.65 and -0.14 . We test now, in the second step, whether the enlargement of the second segment of the right hand would result in a more stable segment.

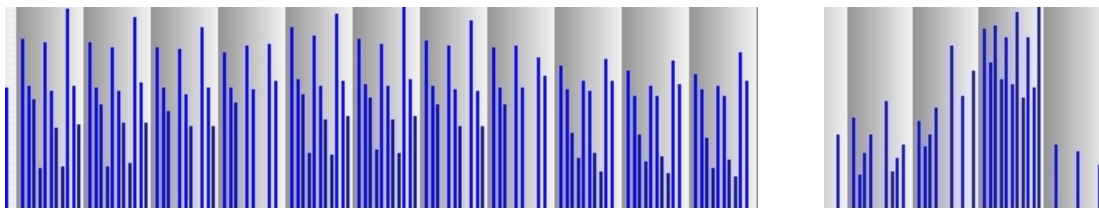


Figure 8.30. Left: Metric weight $W_{2,2}$ of first segment candidate (Bars 1–11). Right: Metric weight $W_{2,2}$ of second segment candidate (Bars 12–15).

Shifting the boundary by one bar to the left results in a metric weight pattern for Bars 11–15 (see Figure 8.31) that is characterized by peaks on the 2nd, 5th, 8th, and 11th eighth notes in Bars 11, 12, and the first half of Bar 13. Hence, the enlargement of the second segment might result in greater stability characterized by layers in the metric weight.

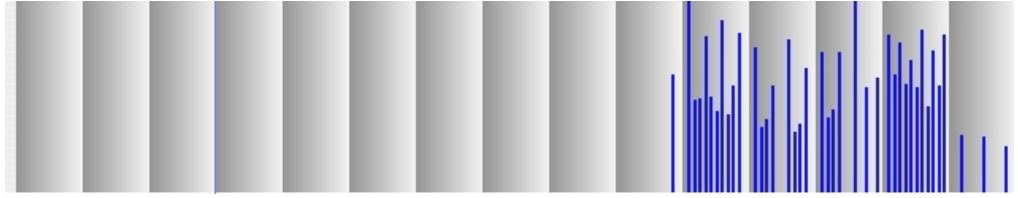


Figure 8.31. Extension of the second segment candidate by one bar: the segment candidate of Bars 11–15.

In order to obtain a stable-as-possible second segment we shift the beginning of this segment candidate increasingly further to the left. Figure 8.32 shows, from top to bottom, the process of shifting the beginning by one Bar to the left. We thus incrementally add to the segment candidate Bars 11–15 the segment candidates Bars 10–15, Bars 9–15, Bars 8–15, and Bars 7–15.

Starting with the first extended segment of Bars 11–15, we obtain regions within these new segment candidates that are characterized by peaks of the metric weights at the 2nd, 5th, 8th, and 11th eighth notes. Furthermore, the metric weights of the last two segment candidates (Bars 8–15, Bars 7–15) in Figure 8.32 demonstrate that shifting the second segment beyond Bar 9 results in a drastic decrease of the metric weights before Bar 9. In the last segment candidate in Figure 8.32, consisting of Bars 7–15, the characteristic high metric weights on the 2nd, 5th, 8th, and 11th eighth notes are also weakened after Bar 9. Furthermore, Bar 7 again reveals three peaks at the 2nd, 6th, and 10th eighth notes, as observed in the first segment of Bars 1–11. This suggests that the most stable second segment out of these candidates can be obtained by choosing Bars 9–15.

In order to test this assumption with the correlation coefficient values, we display the corresponding values of metric weights of consecutive bars for all segment candidates in Figure 8.33 from left to right. While none of the correlation coefficients of the original segment candidate Bars 12–15 reaches the value of 0.7, the greatest correlation coefficient value of segment candidate Bars 11–15 is already higher than 0.8 at the first data point. The next segment candidate, Bars 10–15, contains two correlation coefficient values above 0.8. The segment candidate Bars 9–15 contains three values above 0.8. In all cases these highest values are located at the beginning of the segment, while the last three values for each segment remain low. In contrast to this, the segment candidate of Bars 8–15 starts with a lower value of 0.5 before the correlation coefficient values increase; the last segment candidate, Bars 7–15, starts with two low values. While the correlation coefficient values did increase in the beginning of all segment candidates—Bars 11–15, Bars 10–15, and Bars 9–15—the extension beyond Bar 9 results again in a decrease of the correlation coefficient values of the beginnings of the segment candidates. This confirms that the beginning of the second segment of the piece should be located at the boundary between Bar 8 and Bar 9. However, the

correlation coefficient values of the very last Bars in each segment candidate could not be increased.

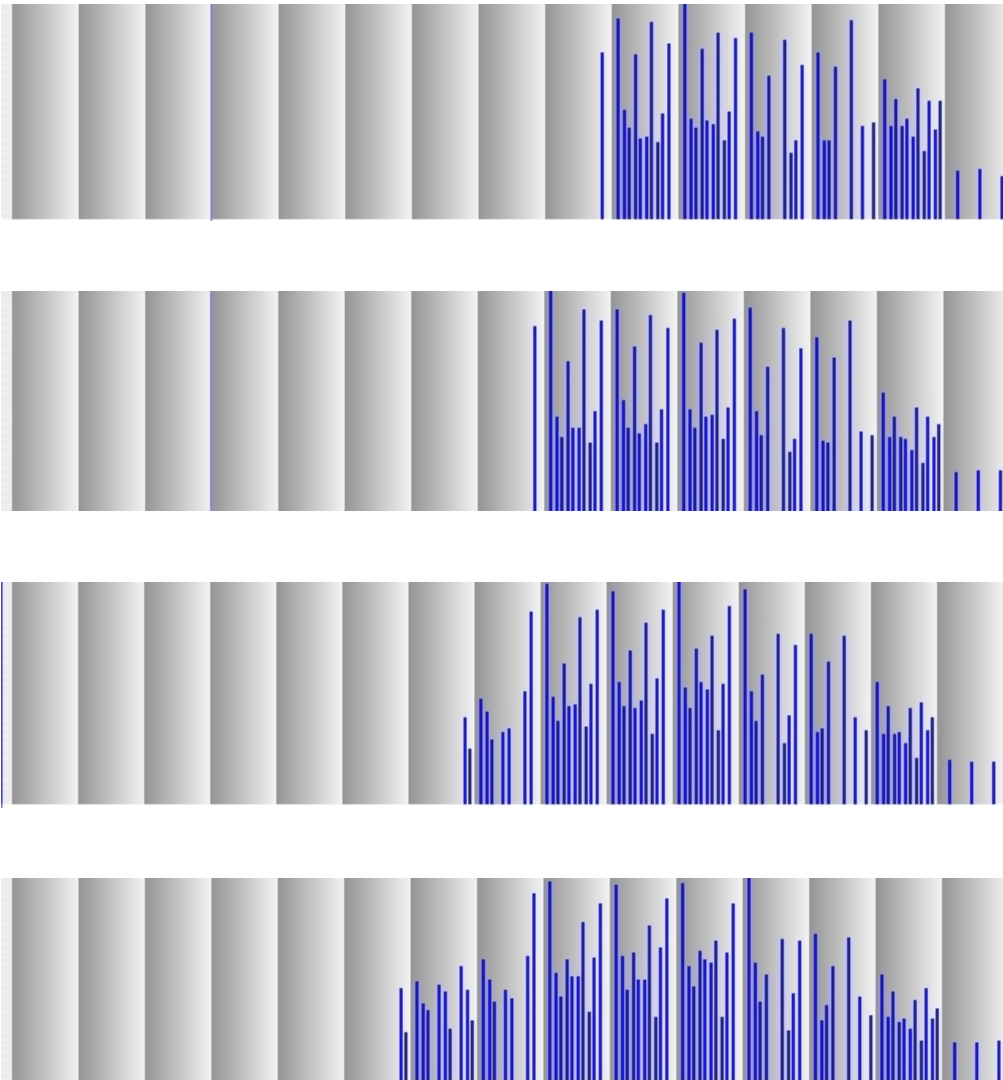


Figure 8.32. Extending the second segment candidate of Bars 12–15 by shifting the beginning backwards: metric weights $W_{2,2}$ of Bars 10–15, Bars 9–15, Bars 8–15, Bars 7–15 (from top to bottom).

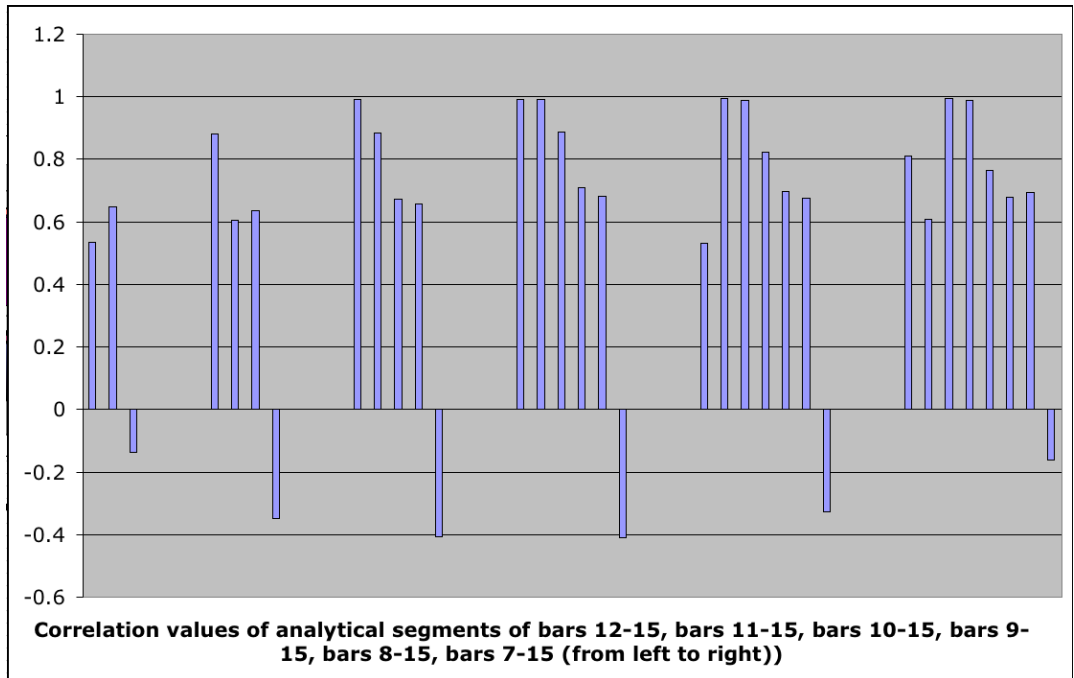


Figure 8.33. Correlation between weights of consecutive bars of the metric weights $W_{2,2}$ of Bars 12-15, Bars 11-15, Bars 10-15, Bars 9-15, Bars 8-15, Bars 7-15 (from left to right).

Hence, even after choosing Bars 9-15 as the best second segment, this segment still contains an unstable region, namely the last two and a half bars, that is not characterized by peaks on the 2nd, 5th, 8th, and 11th eighth notes, as in the first part of this segment. This corresponds on the one hand to the unstable last two bars in the metric weight of the left hand part, and on the other to Lewin's assignment of a metric modulation within these bars. The very first segment candidate of Bars 12-15 obtained within the first step of our segmentation process was not characterized by stable weight layers. In contrast, the metric weights of Bars 12 and 13 within the segment of 9-15 are now characterized by the same metric weight layers as Bars 9-11, and are part of a stable metric region.

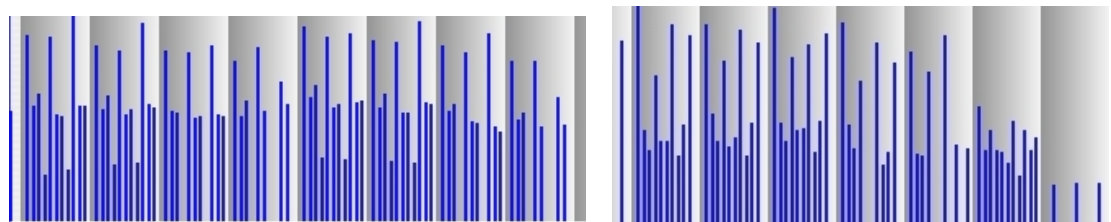


Figure 8.34. Metric weights $W_{2,2}$ of the final segments (Bars 1-8, Bars 9-15).

The comparison of the final segments of Bars 1–8 as the first, and Bars 9–15 as the second segment in Figure 8.34 shows two different metric weight characteristics. The first segment is, in all bars, characterized by peaks on the 2nd, 6th, and 10th eighth notes, while the second segment is characterized by peaks on the 2nd, 5th, 8th, and 11th eighth notes in the first five and a half bars. Hence, the first segment suggests a correspondence to a shifted $3/2$ meter, while the second suggests a correspondence to a shifted $12/8$ meter. The spectral weights in Figure 8.35 confirm that these are indeed the predominant characteristics of these segments.

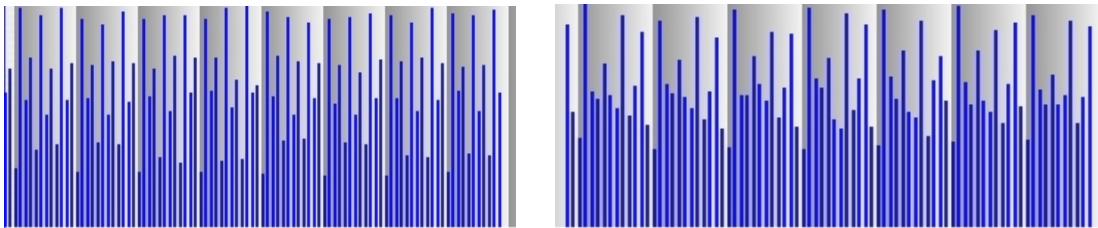


Figure 8.35. Spectral weights $SW_{2,2}$ of the final segments (Bars 1–8, Bars 9–15).

Applying Inner Metric Analysis to the first 15 bars of Brahms' Capriccio leads to the results for which a graphical representation is given in Figure 8.36. In summary, the analysis of both hand parts does not result in a segmentation of Bars 1–15 of the Capriccio. The left hand part is characterized by weight layers corresponding to a $6/4$ meter in the first segment (Bars 1–13) and a transitional unstable segment (Bars 14–15). The right hand is divided into the stable segment of Bars 1–8, characterized by weight layers corresponding to a shifted $3/2$ meter, and a second segment (Bars 9–15), characterized by weight layers corresponding to a $12/8$ meter, which contains a transitional unstable region in Bars 14–15.

8.3.2 Tonal Analysis

In this section, we present the analysis of Brahms' Capriccio using the Argus method as outlined in Section 8.2.5. The score was encoded as a text file such that, for each eighth-note interval, the names of all active pitches are known. The text file was then given as input to the Argus program. The forward and backward windows are set to the same size, $f = b = 12$ eighth notes, that is to say, one bar.

Grazioso ed un poco vivace.
Anmuthig lebhaft.

The image shows a musical score for Brahms' Capriccio, bars 1-15. The score is presented in five systems, each with a different background color for the right hand (treble clef) and a different background color for the left hand (bass clef). The first system (bars 1-8) has a blue background for the right hand and a red background for the left hand. The second system (bars 9-13) has a green background for the right hand and a red background for the left hand. The third system (bars 14-15) has a lighter green background for the right hand and a red background for the left hand. The score includes dynamic markings like 'mp' and 'rit.', and a first ending bracket at the end.

Figure 8.36. Bars 1–15 of Brahms' Capriccio with metric analyses superimposed on score. The blue region [right hand, Bars 1-8] indicates a 3/2 meter, the green region [right hand, Bars 9-13] indicates a 12/8 meter, the red region [left hand, Bars 1-13] indicates a 6/4 meter. The lighter green and red regions [both hands, Bars 14-15] indicate metric modulation areas.

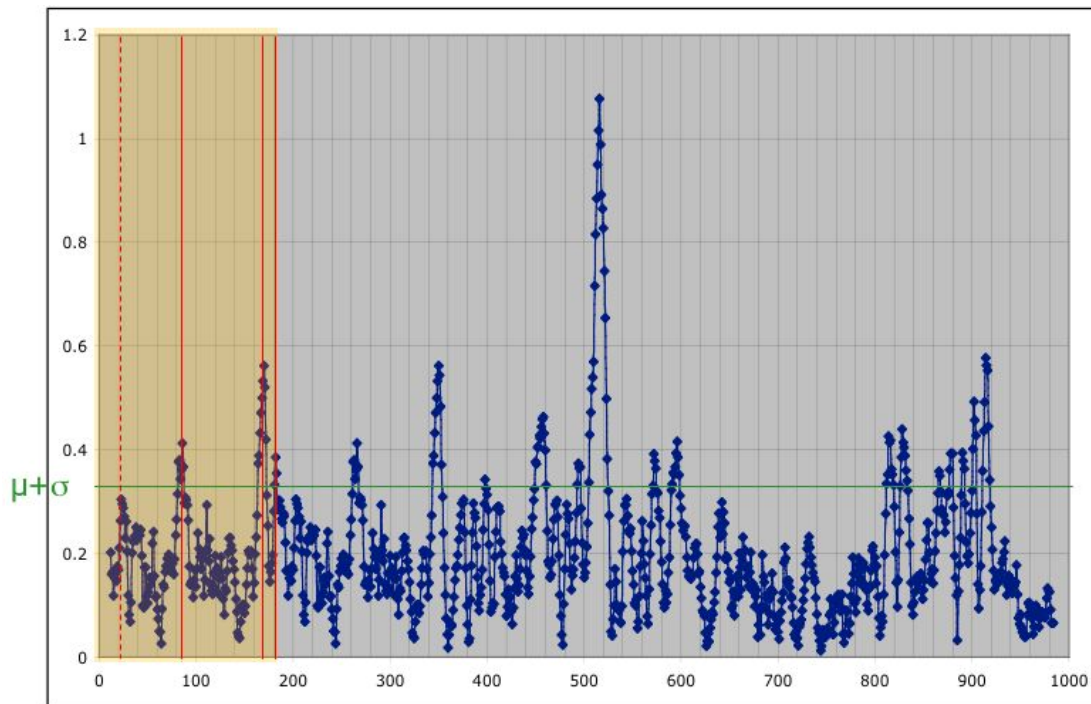


Figure 8.37. Plot of center-of-effect (c.e.) distance values over time [$f = 12$, $b = 12$, $\mu = 0.1987$, $\sigma = 0.1304$].

At each point in time, all the pitches in the forward window are mapped to their corresponding representations in the Spiral Array, and the program computes the position of the center-of-effect of these pitches, a sum of the pitch positions weighted by the relative durations. The same is done in the backward window. The program then calculates the distance between the two centers-of-effect. Figure 8.37 shows the graph of these c.e. distances over time (counted in eighth notes) for the entire piece (including repeats).

The extremely high peak in the middle of the piece occurs at the point where the composer spells the pitches with their enharmonic equivalents, marking a climax of the piece. The highlighted section on the left part of each chart corresponds to Bars 1–15 of the Capriccio, the focus of this paper. The horizontal line marks the level of $\mu + \sigma$ on the chart. Peaks in the highlighted region that are above $\mu + \sigma$ are delineated by solid vertical lines. Peaks below but close to the threshold are delineated by dotted vertical lines.

Figure 8.38 shows the score with the boundaries for tonal change corresponding to those identified in Figure 8.37 marked with similar vertical lines. Consider the three boundaries resulting from this analysis—segment one is from the pickup into Bar 1 through 5/6 of the second bar, segment two is from the sixth quarter of Bar 2

through the end of Bar 7, the third segment ends just before Bar 15, and the final segment is a short one, consisting only of Bar 15.

The Capriccio is written in the key of C, yet never tonicizes in the key throughout the entire first section of the piece. The first boundary divides the initial nebulously C-major region from the equally non-committal F (IV of C) region. Crossing the second boundary leads to an E minor (vii of F, also the relative minor of G) region, and the final boundary leads back to the C region via F.

The image shows the first 15 bars of Brahms' Capriccio in C major. The score is annotated with red text and symbols to indicate tonal boundaries and changes. At the beginning, the tempo is marked "Grazioso ed un poco vivace" and "Anmuthig lebhaft", with a dynamic marking of "mp". A red "C" is placed in the bass clef at the start. A red dashed vertical line with a scissors icon at the top is positioned at the end of bar 7. A red solid vertical line with a scissors icon at the bottom is positioned at the end of bar 14. A red "F" is placed in the bass clef at the end of bar 14. A red "e" is placed in the bass clef at the end of bar 15. A red "F" is placed in the bass clef at the end of bar 15, with a red arrow pointing to a red "C" at the end of the page. The score includes various musical notations such as slurs, accents, and dynamic markings like "sonf." and "p rit."

Figure 8.38. Bars 1–15 of Brahms' Capriccio with tonal analyses superimposed on score.

8.3.3 Comparison

We now compare the metric and tonal analyses with each other, and with Lewin's results. Taking into account that the sections for the tonal analysis often include the preparatory bar prior to a new section, our tonal and metric analyses appear to agree in the second and third boundaries. The second tonal boundary occurs one bar before the corresponding metric boundary. The one-bar difference is due to the fact that the chord in Bar 8, B seventh, serves a dominant function leading to the upcoming region in e minor, which is termed the dominant-substitute key region in Lewin's analysis. As a result, the Argus program groups Bar 8 with the e minor segment.

The first tonal boundary, according to the Spiral Array, has no correspondence in the Inner Metric Analysis segmentation, but has a parallel in Lewin's analysis. In Lewin's analysis, the end of the second bar marks the transition between the "tonic" and "subdominant" regions. The Argus result is two eighth notes off from Lewin's. Argus is unaware of bar lines and sequence (and hence melodic pattern) information, and groups the preparatory upbeat into Bar 3 with the second segment.

Inner Metric Analysis is based on equidistant notes' attacks and does not consider pitch information. Lewin's and Cohn's analyses of the Capriccio, on the other hand, are explicitly based on pitch information. Surprisingly, the right hand exhibits a 3/2 metric state within Bars 1–8 in the Inner Metric Analysis results, which include the section of Bars 3–4 labeled by Lewin as 3/2 for the left hand. Furthermore, the right hand is grouped as 12/8 in Bars 9–13 in accordance with Lewin's findings for the left hand. Hence, metric states of the left hand assigned on the basis of pitch information correspond with metric states of the right hand assigned on the basis of time information.

Lewin segments the piece into the "antecedent" section, Bars 1–8 governed by tonicized F harmonies, and the "consequent" section, comprising Bars 9–15 governed by tonicized e harmonies. Inner Metric Analysis splits the example into the first and second half, agreeing with Lewin's main sections. The tonal analysis using the Spiral Array gives the division between Lewin's "tonic" and "subdominant" regions in the antecedent section, and between the "tonic" and "dominant" regions between the antecedent and consequent sections.

Bars 14–15 contain a metric modulation, according to Lewin. The metric model also shows a modulation from 12/8 back to 3/2 in the right hand and a transitional region in the left hand; the Spiral Array analysis shows a boundary from e minor to F, leading back to the tonic, C. We have shown similarities in the results for corresponding sections of the mathematical models for metric and tonal domains with Lewin's and Cohn's findings, thus providing further evidence for the affinity between tonal and metric structures in Brahms' Op. 76, No. 8.

8.4 Conclusions

We have presented independent methods for meter and tonal induction through the Inner Metric Analysis and Spiral Array models respectively. We then introduced the Argus method for tracking tonal change over time, and a corresponding method for determining metric change over time. In the metric realm, we put forth a sensitivity analysis technique for testing the stability of a segmentation result. The methods were illustrated by numerous examples from various composers. In particular, we applied these methods to Brahms' Capriccio to independently segment the example into metrically stable and tonally stable sections. The comparison of the computational results of these models supports what Lewin and Cohn have found: there is a close relationship between harmony and meter in Brahms' Op.76, No.8.

Acknowledgments

This material is based upon work supported by a Women in Science and Engineering (WiSE) Postdoctoral Fellowship and National Science Foundation (NSF) Grant No. 0347988. The work made use of the Integrated Media Systems Center Shared Facilities, supported by the National Science Foundation under Cooperative Agreement No. EEC-9529152. Any opinions, findings, conclusions, or recommendations expressed in this material are those of the authors and do not necessarily reflect the views of WiSE or NSF.

References

- Caplin, William (1983). "Tonal Function and Metrical Accent: A Historical Perspective," *Music Theory Spectrum* (5), 1–14.
- Chew, Elaine (2000). *Towards a Mathematical Model of Tonality*. Ph.D. dissertation, Operations Research Center, MIT, Cambridge, MA.
- Chew, Elaine (2001). "Modeling Tonality: Applications to Music Cognition," in *Proceedings of the 23rd Annual Meeting of the Cognitive Science Society*, ed. Johanna D. Moore and Keith Stenning (Mahwah, NJ: Lawrence Erlbaum Associates), 206–11.
- Chew, Elaine (2002). "The Spiral Array: An Algorithm for Determining Key Boundaries," in *Music and Artificial Intelligence, Proceedings of the Second International Conference*, ed. Christina Anagnostopoulou, Miguel Ferrand, and Alan Smaill (Berlin: Springer-Verlag), 18–31.
- Chew, Elaine (2004). "Regards on Two Regards by Messiaen: Automatic Segmentation Using the Spiral Array," in *Proceedings of the Sound, Music and Computing (SMC '04) Conference* (Paris, France).
- Chew, Elaine and Yung-Cheng Chen (2005). "Real-Time Pitch Spelling Using the Spiral Array," *Computer Music Journal* (29:2), 61–76.
- Chew, Elaine (2006a). "Slicing It All Ways: Mathematical Models for Tonal Induction, Approximation and Segmentation Using the Spiral Array," *INFORMS Journal on Computing*, Special Cluster on Computation in Music, ed. Elaine Chew, Roger Dannenberg, Joel Sokol, and Mark Steedman, (18:3), 305–20.
- Chew, Elaine (2006b). "Regards on Two Regards by Messiaen: Post-tonal Music Segmentation Using Pitch Context Distances in the Spiral Array," *Journal of New Music Research*, Special

- Issue on Sound and Music Computing, selected papers from the First Sound and Music Computing Conference, revised and expanded, ed. Gérard Assayag, (34:4), 341–54.
- Chuan, Ching-Hua and Elaine Chew (2007). "Audio Key Finding: Considerations in System Design, and the Selecting and Evaluating of Solutions," *EURASIP Special Issue on Music Information Retrieval Based on Signal Processing*, ed. Ichiro Fujinaga, Masataka Goto, and George Tzanetakis, (Article ID 56561), 15 pages.
- Cohn, Richard (2001). "Complex Hemiolas, Ski-Hill Graphs, and Metric Spaces," *Music Analysis* (20:iii), 295–326.
- Eck, Douglas (2002). "Finding Downbeats with a Relaxation Oscillator," *Psychological Research* (66), 18–25.
- Epstein, David (1987). *Beyond Orpheus* (Oxford, UK: Oxford University Press).
- Fleischer, Anja, Guerino Mazzola, and Thomas Noll (2000). "Computergestützte Musiktheorie," *Musiktheorie* (4), 314–25.
- Fleischer, Anja (2002). "A Model of Metric Coherence," in *Proceedings of the 2nd Conference Understanding and Creating Music* (Caserta, Italy).
- Fleischer, Anja (2003). *Die analytische Interpretation, Schritte zur Erschließung eines Forschungsfeldes am Beispiel der Metrik* (available on the internet from dissertation.de, Berlin).
- Frisch, Walter (1990). "The Shifting Barline: Metrical Displacement in Brahms," in Bozarth, G. S. (ed.): *Brahms Studies*, 139–63 (Oxford: Clarendon Press).
- Gómez, Emilia (2006). "Tonal Description of Polyphonic Audio for Music Content Processing," *INFORMS Journal on Computing*, Special Cluster on Computation in Music, ed. Elaine Chew, Roger Dannenberg, Joel Sokol, and Mark Steedman, (18:3), 294–304.
- Honingh, Aline (2007). "Automatic Modulation-Finding Using Convex Sets of Notes," in *Proceedings of the International Conference on Mathematics and Computation in Music* (Berlin, Germany).
- Izmirli, Ozgur (2005). "An Algorithm For Audio Key Finding," in Extended Abstracts of the 1st Annual Music Information Retrieval Evaluation eXchange (London, UK).
- Krebs, Harald (1999). *Fantasy Pieces* (Oxford, UK: Oxford University Press).
- Krumhansl, Carol (1990). *Cognitive Foundations of Musical Pitch* (Oxford, UK: Oxford University Press).
- Large, Edward W., and John F. Kolen, (1994). "Resonance and the Perception of Musical Meter," *Connection Science* (6), 177–208.
- Large, Edward W. (2000). "On Synchronizing Movements to Music," *Human Movement Science* (19), 527–66.
- Lerdahl, Fred, and Ray Jackendoff (1983). *A Generative Theory of Tonal Music* (Cambridge, MA: MIT Press).
- Lewin, David (1981). "On Harmony and Meter in Brahms's Op.76, No.8," *19th-Century Music* (4:3), 261–5.
- Longuet-Higgins, H. Christopher, and Christopher Lee (1987). "The Rhythmic Interpretation of Monophonic Music," *Mental Processes*, 150–68, (Cambridge, MA: MIT Press).
- Longuet-Higgins, H. Christopher, and Mark J. Steedman (1971). "On Interpreting Bach," *Machine Intelligence* (6), 221–41.
- Mazzola, Guerino (2002). *The Topos of Music* (Basel: Birkhäuser).
- McAuley, J. Devin (1994). "Finding Metrical Structure in Time," in *Proceedings of the 1993 Connectionist Models Summer School*, 219–27.

- Nestke, Andreas, and Thomas Noll (2001). "Inner Metric Analysis," *Music and Mathematics*, ed. J. Haluska (Bratislava: Tatra Mountains Publications), 91–111.
- Phipps, Graham (2001). "Die Überleitung in der Sonatenhauptsatzform. Auf den Spuren Martin Heideggers im ersten Satz der II. Sinfonie von Brahms," talk given at the *Congress of the German Society of Music Theory* in Dresden, December 9.
- Raphael, Christopher (2001). "Automated Rhythm Description," in *Proceedings of the 2nd Annual International Symposium on Music Information Retrieval* (Bloomington, IN: Indiana University), 99–107.
- Povel, Dirk-Jan, and Peter Essens (1985). "Perception of Temporal Patterns," *Music Perception* (2), 411–40.
- Rizo, David, and José M. Iñesta (2005). "Tree Symbolic Music Representation for Key Finding," in *Extended Abstracts of the 1st Annual Music Information Retrieval Evaluation eXchange* (London, UK).
- Sapp, Craig (2001). "Harmonic Visualizations of Tonal Music," in *Proceedings of the International Computer Music Conference* (Havana, Cuba), 423–30.
- Shmulevich, Ilya and Olli Yli-Harja, "Localized Key Finding: Algorithms and Applications," *Music Perception* (17:4), 531–44.
- Schoenberg, Arnold (1976). "Stil und Gedanke," *Gesammelte Schriften*, ed. I. Vojtech, Volume 1 (Frankfurt/Main: S. Fischer), 35–71.
- Steedman, Mark (1977). "The Perception of Musical Rhythm and Meter," *Quarterly Journal of Experimental Psychology* (6), 555–69.
- Temperley, David (1999). "What's Key for Key? The Krumhansl-Schmuckler Key-Finding Algorithm Reconsidered," *Music Perception* (17:1), 65–100.
- Temperley, David (2001). *The Cognition of Basic Musical Structures* (Cambridge, MA: MIT Press).
- Temperley, David (2002). "A Bayesian Approach to Key Finding," in *Music and Artificial Intelligence, Proceedings of the Second International Conference*, ed. Christina Anagnostopoulou, Miguel Ferrand, and Alan Smaill (Berlin: Springer-Verlag), 195–206.
- Toiviainen, Peter, and Tuomas Eerola (2004). "The Role of Accent Periodicities in Meter Induction: A Classification Study," in *Proceedings of the 8th International Conference on Music Perception and Cognition* (Evanston, IL), 422–5.
- Toiviainen, Petri and Carol L. Krumhansl (2003). "Measuring and Modeling Real-Time Responses to Music: the Dynamics of Tonality Induction," *Perception* (32:6), 741–66.
- Volk, Anja (2004). "Metric Investigations in Brahms' Symphonies," *Perspectives of Mathematical and Computational Music Theory*, ed. Guerino Mazzola, Thomas Noll, and Emilio Lluis-Puebla (Osnabrück: epOs Music), 300–29.
- Yeston, Maurice (1976). *The Stratification of Musical Rhythm* (New Haven, CT: Yale University Press).

Submitted: 7 November 2005. Final revisions: 31 August 2007.